HOKKAIDO UNIVERSITY

Title	Technical note : Point-by-point ion-recombination correction for accurate dose profile measurement in high dose-per-pulse irradiation field
Author(s)	Kojima, Hideki; Ishikawa, Masayori; Takigami, Makoto
Citation	Medical physics, 50(11), 7281-7293 https://doi.org/10.1002/mp.16641
Issue Date	2023-08-01
Doc URL	https://hdl.handle.net/2115/95805
Rights	This is the peer reviewed version of the following article: Technical note: Point - by - point ion - recombination correction for accurate dose profile measurement in high dose - per - pulse irradiation field, 50(11) pp7281-7293 2023, which has been published in final form at https://doi.org/10.1002/mp.16641. This article may be used for non-commercial purposes in accordance with Wiley Terms and Conditions for Use of Self-Archived Versions. This article may not be enhanced, enriched or otherwise transformed into a derivative work, without express permission from Wiley or by statutory rights under applicable legislation. Copyright notices must not be removed, obscured or modified. The article must be linked to Wiley's version of record on Wiley Online Library and any embedding, framing or otherwise making available the article or pages thereof by third parties from platforms, services and websites other than Wiley Online Library must be prohibited.
Type	journal article
File Information	230908_Medical_Physics_Kojima_Final_Manuscript(For_HUSCAP).pdf

Hokkaido University Collection of Scholarly and Academic Papers : HUSCAP

Technical Note: Point-by-point ion-recombination correction for accurate dose profile measurement in high dose-per-pulse irradiation field

Running title: Ion-recombination correction for PDD

Authors:

Hideki Kojima, Masayori Ishikawa* and Makoto Takigami.

Authors and affiliations:

Hideki Kojima

Department of Radiation Oncology, Sapporo Higashi Tokushukai Hospital, Sapporo, Hokkaido, Japan

Masayori Ishikawa, Ph.D.

Graduate School of Health Sciences, Hokkaido University, Sapporo, Hokkaido, Japan

Makoto Takigami

Department of Radiation Technology, KKR Sapporo Medical Center, Sapporo, Hokkaido, Japan

* Corresponding author: Masayori Ishikawa (masayori@med.hokudai.ac.jp)

ABSTRACT

Background: Although flattening filter free (FFF) beams are commonly used in clinical treatment, the accuracy of dose measurements in FFF beams has been questioned. Higher dose per pulse (DPP) such as FFF beams from a linear accelerator may cause problems in dose profile measurements using an ionization chamber due to the change of the charge collection efficiency. Ionization chambers are commonly used for percent depth dose (PDD) measurements. Changes of DPP due to chamber movement during PDD measurement can vary the ion collection efficiency of ionization chambers. In the case of FF beams, the DPP fluctuation is negligible, but in the case of the FFF beams, the DPP is 2.5~4 times larger than that of the FF beam, and the change in ion collection efficiency is larger than that of the FF beam. PDD profile normalized by maximum dose depth, 10 cm depth for example, may therefore be affected by the ion collection efficiency.

Purpose: In this study, we investigate the characteristics of the ion collection efficiency change depending on the DPP of each ionization chamber in the FFF beam. We furthermore propose a method to obtain the chamber-independent PDD by applying a DPP-dependent ion recombination correction.

Methods: Prior to investigating the relationship between DPP and charge collection efficiency, Jaffe-plots were generated with different DPP settings to investigate the linearity between the applied voltage and collected charge. The absolute dose measurement using 8 ionization chambers under the irradiation settings of 0.148, 0.087, and 0.008 cGy/pulse were performed. Applied voltages for the Jaffe-plots were 100, 125, 150, 200, 250 and 300 V. The ion recombination correction factor P_{ion} was calculated by the two-voltage analysis (TVA) method at the applied voltages of 300 V and 100 V. The DPP dependency of the charge collection efficiency for each ionization chamber were evaluated from the DPP- P_{ion} plot. PDD profiles for the 10 MV FFF beam were measured using Farmer type chambers (TN30013, FC65-P and FC65-G) and mini-type chambers (TN31010, TN31021, CC13, CC04 and FC23-C). The PDD profiles were corrected with ion recombination correction at negative and positive polar applied voltages of 100 V and 300 V.

Results: From the DPP-P_{ion} relation for each ionization chamber with DPP ranging from 0.008 cGy/pulse to 0.148 cGy/pulse, all Farmer and mini-type chambers satisfied the requirements described in AAPM TG-51 addendum. However, P_{ion} for the CC13 was most affected by DPP among tested chambers. The maximum deviation among PDDs using 8 ionization chambers for 10 MV FFF was about 1%, but the deviation was suppressed to about 0.5% by applying ion recombination correction at each depth.

Conclusions: In this study, the deviation of PDD profile among the ionization chambers was reduced by the ion recombination coefficient including the DPP dependency, especially for high DPP beams such as FFF beams. The present method is particularly effective for CC13, where the ion collection efficiency is highly DPP dependent.

Key words: Ion-recombination correction, Dose profile measurement, Dose per pulse

1. Introduction

Accurate beam profile measurement has become in recent years one of the most important components of high-precision radiation therapy[1,2,7]. Calculation accuracy of the radiation treatment planning system (RTPS) is affected by the quality of the obtained beam profile[3-6]. Measured beam data are used for beam modeling to reproduce machine characteristics such as photon/electron radial energy distributions, fluence distribution, percentage depth dose (PDD) and beam profile. Among these characteristics, PDD and beam profile measurements are usually acquired by each institute. Higher accuracy for these beam data measurements is desirable for more accurate dose calculations in the RTPS[7]. The characteristics of the detector are important for the accuracy in depth profile measurements[8,30]. Ionization chambers, for example, with low energy dependence are desirable in measuring PDDs[7].

VARIAN TrueBeam linacs (Varian Medical Systems, Palo Alto, CA, USA) are equipped with a flattening filter free (FFF) beam in addition to the conventional flattening filter (FF) beam. The FFF beam has 2.5 to 4 times higher dose per pulse (DPP) compared to that of the FF beam. The nominal DPP for the 6 and 10 MV FF beams of TrueBeam linacs is 0.03 cGy/pulse at the maximum dose depth with a 10×10 cm^2 irradiation field, while those for the 6 and 10 MV FFF beams are 0.08 and 0.13 cGy/pulse, respectively. The dose rates in TrueBeam linacs are controlled by skipping certain beam pulses[12,20,21,33], so the DPP does not depend on the beam dose rate (MU/min). On the other hand, DPP affects the ion collection efficiency in dosimetry with ionization chambers in the pulse beam of linear accelerators[9-14,20,23-26].

The deviation of ion collection efficiency by ionization chamber type is not negligible for FFF beams. The DPP of the FFF beam varies greatly with the depth of the water. On the other hand, studies on the variation of ion collection efficiency by ionization chamber in FFF beams have been performed at a certain depth (e.g., 10 cm), but there is no report on the change in ion collection efficiency during PDD measurement. Since the change in ion collection efficiency due to high DPP beam such as FFF beam should be different among ionization chambers, the beam profile for FFF beam may be different depending on ionization chamber used for the profile measurement.

In this study, we investigate the ion collection efficiency change during depth dose profile measurements for several ionization chambers and propose a practical ion-recombination correction method to obtain equally accurate PDD profiles even if using different ionization chambers.

2. Materials and Methods

2.A. Ionization chambers

Eight ionization chambers were used in this study: Farmer-type, TN30013 (PTW, Freiburg, Germany), FC65-G (IBA Dosimetry, Schwarzenbruck, Germany), FC65-P (IBA Dosimetry), mini-type, TN31010 (PTW), TN31021 (PTW), CC13 (IBA Dosimetry), FC23-C (IBA Dosimetry), CC04 (IBA Dosimetry). A 3D water phantom, Blue Phantom2 (IBA Dosimetry) was employed for all measurements. The electrometer employed in the study was RAMTEC Smart (Toyo Medic, Tokyo, Japan). For polarizing voltage, a positive voltage was applied to the center electrode and the electron charge was collected from the center electrode, unless otherwise specified[13]. The applied voltages in the figures and tables are unified by the polarity of the center electrode.

2.B. DPP dose rate evaluation

Varian TrueBeam was used for all experiments in this study. In this linac, the FFF beam is controlled by the pulse drop method, which stabilizes the dose rate by skipping some beam pulses during irradiation[12,20,21,33]. Since the number of pulses in the beam is essential for accurate DPP measurement, an in-house pulse counter was used for counting the beam pulses during irradiation. The pulse counter was connected to an AFC TRIG (J17) connector in the console control cabinet of the TrueBeam. TrueBeam 2.7 or later has an output for the beam pulse signal. Accurate counts of the beam pulse are easily obtained by connecting to this J17 connector[32)]. For the absolute DPP measurement, a Farmer-type ionization chamber (TN30013, PTW) and a scanning water phantom (Blue Phantom2, IBA Dosimetry) were used. The absolute DPP (cGy/pulse) was calculated from the absolute dose of 1000 MU irradiation divided by the measured beam pulse counts. For obtaining various DPPs, 10 patterns of DPP irradiation settings were set as shown in Table 1. Among the irradiation settings, 4 and 6 MV FF beams were used for 0.008 and 0.022 cGy/pulse, respectively, and 10 MV FFF beams were used for all other settings. The absorbed dose was calculated according to IAEA TRS-483[1]. The DPPs ranged from 0.008 to 0.148 (cGy/pulse). The ratio of maximum DPP to minimum DPP is 18.5.

2.C. DPP dependent ion recombination correction

2.C.1 Ion recombination correction formula

Cylindrical ionization chambers are commonly used in dosimetry for high-energy X-ray radiotherapy. An electric field gradient between the center electrode and the cavity wall depends on the applied polarizing voltage to the ionization chamber[13,23] and the charge collection efficiency depends on the electric field gradient. Electron loss frequently occurs at lower applied voltages due to ion recombination. On the other hand, electron generation occurs at higher applied polarizing voltages due to electron avalanche. Various methods for calculating ion recombination have been reported in previous studies such as theoretical estimation from detector dimensions, direct estimation by measurement, etc.[9-13,17,18,20-26]. The most accepted method for estimating the ion recombination correction factor is substituting the measured value of the actual beam into an approximate equation[1,8,15,16,19], whose typical method is the TVA (two voltage analysis) method[8-12,16-26]. The TRS-398 published by the International Atomic Energy Agency (IAEA) recommends use of the TVA method for estimation of ion recombination correction factor k_s which can be obtained by the following formula[16]:

$$k_S = a_0 + a_1\left(\frac{Q_H}{Q_L}\right) + a_2\left(\frac{Q_H}{Q_L}\right)^2 \qquad (1)$$

where Q_H and Q_L are the charges measured at different applied polarizing voltages V_H, V_L, respectively. Coefficients of a_0, a_1, and a_2 are determined by the ratio V_H / V_L of the two applied polarizing voltages. For these coefficients, TRS-398 adopts the value of Weinhous[18] and recommends that V_H/V_L should be larger than 3.0.

On the other hand, in AAPM TG-51[19,8] the ion recombination correction factor P_{ion} is deduced from the virtual charge Q_∞ at infinite voltage which can be obtained by a linear extrapolation from the relationship between the charge measured by TVA and the applied polarizing voltage. The ion recombination correction factor $P_{ion}(V_H)$ for the high voltage V_H is obtained by the following equation (2):

$$P_{ion}(V_H) = \frac{1-\frac{V_H}{V_L}}{Q_H/Q_L - V_H/V_L} \quad (2)$$

where the high voltage is V_H, the low voltage is V_L, and Q_H and Q_L are the charge quantities measured at the voltages of V_H and V_L, respectively.

As in Eqs. (1) and (2), when linearity is observed between multiple applied voltages and collected charges within a certain range of rated applied voltages, multi-voltage analysis (MVA) can be used.[12,25] The virtual charge (Q_∞) at the maximum ion collection efficiency is often obtained by extrapolation using Jaffe-plots. Exploiting this by letting $V^{-1} \rightarrow 0$, one finds Q_∞ from which the recombination factor can be found. Using Q_∞ to define the ion recombination correction factor $P_{ion}(V_M)$ using Q_∞ is expressed by the following equation:

$$P_{ion}(V_M) = \frac{Q_\infty}{Q} \quad (3)$$

where Q_∞ and Q are the saturation charge current and the measured charge current at polarizing voltage V_M, respectively. Q_∞ denotes the ion collection efficiency of 100%, i.e., infinite voltage, and $V^{-1} \rightarrow 0$ is the same as with the TVA method. In Eqs. (1) and (2) the ion recombination correction factor can be calculated only for high voltage (V_H) used in measurement, while in Eq. (3), P_{ion} can be calculated for all applied polarizing voltages.

2.C.2 DPP dependent Jaffe-Plots

Prior to investigating the relationship between DPP and charge collection efficiency, Jaffe-plot measurements were performed with different DPP settings to investigate the linearity between the applied voltage and collected charge. The absolute dose measurement using 8 ionization chambers under the irradiation settings of 0.148, 0.087, and 0.008 cGy/pulse were performed. Applied voltages for the Jaffe-plots were 100, 125, 150, 200, 250 and 300 V.

The ion recombination correction factor P_{ion} was calculated by the TVA method (Eq. (2)) at the applied voltages of 300 V and 100 V. The DPP dependency of the charge collection efficiency for each ionization chamber were evaluated from the DPP- P_{ion} plot.

2.D. Depth dose profile with and without ion recombination correction

In order to apply ion recombination correction for the depth dose profile measurement, PDD measurement with two polarizing voltages of 100 V and 300 V were performed (Fig. 1(a)). We applied ion recombination correction not to the integral charge but to the average current because the average current includes dose rate information. The ion recombination correction coefficients for k_S using Eq. (1) and P_{ion} using Eq. (2) were calculated at deeper depth than the depth at maximum current because the PDD profile at the surface changes drastically. For example, as shown in Fig. 1(b), k_s can be expressed as a function of measured depth by curve fitting. Finally, as shown in Fig 1(c), corrected measured current can be converted from original measured current using the ion recombination correction function.

PDD profiles for the 10 MV FFF beam were measured using Farmer type chambers (TN30013, FC65-P and FC65-G) and mini-type chambers (TN31010, TN31021, CC13, CC04 and FC23-C). The PDD profiles were corrected with ion recombination correction by equations (1) and (2) at negative and positive polar applied voltages of 100 V and 300 V.

3. RESULTS

3.A. DPP dependent ion recombination correction

Figure 2 shows Jaffe-plots of FC23-C as representative of mini-type and TN30013 as representative of Farmer-type chambers, respectively, at 0.148, 0.087 and 0.008 cGy/pulse. The applied voltage of Jaffe-plots ranged from 100 to 300 V. The inverse of the collected charge Q, 1/Q, is normalized to the charge at 100 V, $1/Q_{100V}$. The Farmer and mini-type ionization chambers all showed good linearity between 100 V and 300 V. Fig. 2(a) and (b) show the Jaffe-plots of FC23-C with positive and negative polar applied voltage, respectively. The coefficient of determination R^2 in the linear approximation of the Jaffe-plot of the FC23-C for all DPPs was $R^2 > 0.99$. As shown in Fig. 2(c)(d), the gradients of the Jaffe-plots for the TN30013 chamber were smaller than FC23, and the TN30013 chamber had good linearity ($R^2 = 1.0$). Other Farmer-type chambers (FC65-P, FC65-G) also had good linearity.

The ion recombination correction factor P_{ion} for each ionization chamber was measured under the settings listed in Table 1. Fig. 3(a) shows the DPP-P_{ion} plots for each ionization chambers with DPP ranging from 0.008 cGy/pulse to 0.148 cGy/pulse. Table 2 shows characteristics of linear approximation for DPP dependency of P_{ion} obtained from Fig. 3(a). The slope of CC13 was the largest among all chambers. AAPM TG-51 Addendum advocates the intercept should be less than 1.002 as a requirement for reference-class ionization chambers.[8,13] As shown in Table 2, these criteria were satisfied for Farmer and mini-type chamber. Fig. 3(b) shows a comparison with the value published in a previous study by Hyun[14] and McEwen et al.[13]. The agreement for TN30013 was within 0.16% (McEwen). The agreement for CC13 was within 0.62% (Hyun) and within 0.08% (McEwen).

3.B. PDD profile measurement with and without ion recombination correction

Figure 4 shows the original PDD and PDD with ion recombination correction by equations (1) and (2) at negative polar applied voltage. Figs. 4(a) - 4(c) show original PDD, corrected $PDD_{(1)}$ and corrected $PDD_{(2)}$, respectively, for the 10 MV FFF beam. Figs. 4(d) - 4(f) show deviations of original PDD, corrected $PDD_{(1)}$ and corrected $PDD_{(2)}$, respectively, from TN30013 for Farmer and mini-type chambers. Figure 5 shows the same original PDD, corrected $PDD_{(1)}$ and corrected $PDD_{(2)}$ at positive applied voltage. Figs. 4(d) and 5(d) show that the deviation of original PDD between the ionization chambers is as large as 1%. The deviation of CC13 is especially large. As shown in Figs. 4(e), 4(f), 5(e) and 5(f), the deviation of the PDD with the ion recombination correction is reduced to 0.5%. Figure 6 shows the same original PDD, corrected $PDD_{(1)}$ and corrected $PDD_{(2)}$ normalized at 10 cm depth with negative polar applied voltage, and Fig. 7 shows the same with positive polar applied voltage.

The original PDD in Figs. 4-7 show that the maximum deviation between ionization chambers is about 1%. In particular, the deviation of CC13 from TN30013 was the largest among all chambers. The corrected $PDD_{(1)}$ and $PDD_{(2)}$ for Farmer and mini-type ionization chambers converged within 0.5% regardless of the applied polarizing voltages. The ion recombination correction effectively reduced the deviation between ionization chambers, especially drastic for CC13. These discrepancies are not caused by the increase in water depth, but by the shallow depth region, i.e., the high DPP. The validity of this consideration is reflected in the results normalized by 10 cm depth. The original PDD of CC13 shows a relative decrease in charge collection near the depth at maximum dose, where it is high at DPP (Fig. 6(d) and Fig. 7(d)), then the deviation becomes higher as the water depth increases. The reason is because

the high DPP reduces the efficiency of charge collection. By applying the ion recombination correction as shown in Fig. 6(e), 6(f), 7(e) and 7(f), the decrease in charge collection around the depth of maximum dose is adequately corrected and the deviation among all chambers is suppressed.

4. DISCUSSION

As shown in Fig. 2(a, b, c, d), all the Farmer and mini-type chambers have good linearity at the applied voltage of 100-300 V with independence of the change of DPP. The ion recombination correction coefficients k_{S_MVA} calculated by MVA, k_{S_TVA} by TVA (Eq. 1), and P_{ion} (Eq. 2) were 1.025, 1.024, and 1.025, respectively, at the applied voltage of 300 V and DPP of 0.148 cGy/Pulse. The deviations between k_{S_MVA}, k_{S_TVA}, and P_{ion} were at most 0.02%, indicating that these ion recombination correction factors are almost equal under the good linearity showed in the Jaffe-plots[12,25]. Equation (1) is an approximation derived by solving the nonlinear equations by Weinhouse et al.[18]. Equations (1) and (2) agree within 0.3% at the applied voltage ratio of 3.0, which is consistent with our results[19]. On the other hand, Equation (2) calculates the collected charge at infinite voltage V_∞ by extrapolation. This is the same process as the estimation of the ion recombination correction factor by MVA. Therefore, the agreement between them depends on the linearity of Jaffe-plots. In other words, if the linearity between the applied voltage and the collected charge is satisfied, the ion recombination correction coefficients k_{S_MVA} and P_{ion} are almost identical. The results of this study indicate that both methods for the ion recombination correction can be acceptable.

As shown in Fig. 3(a), the relationship between DPP and ion recombination correction coefficients showed good linearity for Farmer and mini-type chambers. On the other hand, the slope of CC13 is larger than that of the other chambers, indicating that the ion recombination correction factor is most affected by DPP. And as shown in Fig. 9, the relationship between the measured current and the corrected current with the ion recombination correction can be fitted with a quadratic function rather than a linear function. This is caused by the nonlinearity of the charge collection efficiency, especially at high DPP, where the charge collection efficiency of the chambers decreases. As shown in Fig 8, in the case of the CC13 chamber with 10 MV FFF beam, the difference between the maximum and the minimum of the ion recombination correction factor was almost 2% for the entire PDD measurement. Among the same mini-type chambers, PTW TN31010, which has a similar cavity volume to CC13, has a smaller DPP dependency on the ion recombination correction factor than the other dosimeters, as shown in Fig. 3. As for the reason for the more significant DPP dependency of CC13 compared to other chambers, it may be due to the difference in detector dimensions and electrode materials. The detector dimensions affect the potential gradient between electrodes which greatly influences the probability of electronic avalanche occurrence. Figure 10 shows the theoretical potential gradient near the center electrode which is calculated from the diameter of the center electrode and the distance between the electrodes for the ionization chambers used in this study. The electric potential gradients near the center electrode of CC13 and 31010 are 1.05 and 1.06 times larger, respectively, while the difference due to the electronic avalanche is estimated to be not so large. On the other hand, the potential gradients of 31021 and CC04 are 1.31 to 1.36 times higher than those of the Farmer-type ionization chambers, indicating that they are more prone to electron avalanche. However, the DPP dependencies of 31021 and CC04 were smaller than the Farmer-type chambers, which means that the electronic avalanche does not affect the DPP dependency. On the other hand, the central electrodes of

CC13 and 31010 are made of C552 (air-equivalent plastic) and aluminum, respectively, and their electrical resistivities are 0.03 Ωm and 2.65×10^{-8} Ωm, respectively, a difference of six orders of magnitude. However, C552 is also used as the central electrode in CC04, but its DPP dependency is very small. This may be because the distance between the electrodes is small and ionic recombination is unlikely to occur in the first place, so the effect may simply not be visible.

In the case of measurement at small DPP such as 6 MV and 10 MV FF beams, the dose rate dependence of charge collection was not a major issue in PDD measurements. However, since the PDD curve is affected by the charge collection it is several times higher than DPP, such as with 10 MV FFF beams, and the deviation from the true curve is not negligible. On the other hand, the deviation can be effectively corrected by applying the ion recombination correction with corrected $PDD_{(1)}$ and corrected $PDD_{(2)}$. As for the differences in the correction methods, k_s (TRS-398) and P_{ion} (TG-51) (Fig. 4 - 7), there is no significant difference. If the inverse of the applied voltage is proportional to the inverse of the collected charge in the Jaffe-plots, MVA and TVA (k_s, P_{ion}) are almost identical. For the ion recombination correction factor at a fixed water depth for FFF beams, Hyun et al.[14] concluded the two-point voltage method (TVA) proposed in AAPM TG-51[19] is useful for FFF beams because the TVA method was almost equivalent to the more rigorous Jaffe-plots-based method (MVA).

Various studies of ion collection efficiency have been conducted for a very small number of fixed DPPs; however, no study has been conducted regarding changing DPP conditions. As mentioned above, charge collection efficiency varies with DPP. In this study, instead of using fixed ion recombination correction coefficients, the actual DPP dependent ion recombination correction function was obtained from the original PDD curves with two different applied voltages.

Chang et al.[27] showed that the mean standard deviation (SD) of PDD for three TrueBeam linacs was within 0.2%, but these measurements were all acquired using CC13 chambers. In addition, Tanaka et al.[28] showed that the discrepancy between the PDDs of TN31010 and CC13 chambers using 14 different TrueBeam linacs was about 0.8% under the condition of 10 MV FFF and irradiation fields of 10×10 cm^2. This result is almost the same as the present study. TrueBeam linacs also provide representative beam data[27] (RBD) as standard for users. The PDD of the RBD is measured by using a CC13 chamber. There is a positive opinion on the use of the RBD for the beam modeling of the facility, stating that the deviation of the RBD from the beam data collected at the facility is less than 1%[29]. On the other hand, Tani et al. compared the beam data and the RBDs of nine measurements with CC13, TN31010, and TN31021 chambers, and found that they agreed within 1%, but the deviation of the calculated dose in the water phantom exceeded 2% for the modeled beam[30]. When the RBD is used for beam modeling, it is not important that the RBD agrees from the measured beam data (MBD) within 1%, but the important question is whether the calculated dose distribution after beam modeling in the RTPS is the same or not regardless of the input beam data sets (RBD, MBD) for beam modeling.

The measured beam data set affects the calculation accuracy in RTPSs. In addition, PDD data significantly affects determining the energy spectrum and other important parameters in beam modeling[30,31]. Since the CC13 chamber has a large DPP dependency in charge collection, the PDD profile of the 10 MV FFF beam deviates from the PDD profile obtained by other ionization chambers by about 1%. This discrepancy can be as large as 2% deviation in the dose calculation in the RTPS. The problem here is the fact that the RBD uses the CC13 chamber. Chang et al.[27] suggest

that due to the relatively large variation of P_{ion} for 10 MV FFF, adequate correction should be considered, especially for treatments with deep-seated tumors. We believe that the present method is useful for RBD measurements.

Since our proposed method eliminates the DPP dependency with the collected charge in measuring the PDD for 10 MV FFF beams, the same PDD can be obtained with any ionization chambers. For the same ionization chamber, ion recombination correction including DPP dependency can be applied from the relation shown in Fig. 1. Therefore, if the PDD measurement of 10×10 cm^2, for example, is performed with positive and negative applied voltages, the number of measurements does not increase because the measurement with the normal negative applied voltage is sufficient for the profile measurement in other irradiation fields.

Table 3 summarizes the uncertainty budget. For estimating inter- and intra- measurement uncertainty, two different measurements were performed using a CC13 ionization chamber: one measurement was repeated 10 times with the same setup (repeat case); the other measurement was re-setup 6 times for each measurement (resetup case). Since measurement uncertainty is expected to depend on the amount of charge, the uncertainty at each measurement position was evaluated as u_{Mes}. The corrected $\mathrm{PDD}_C(d)$ (at depth d [mm]) can be expressed as Eq. (4) using raw charge $\mathrm{Q}_O(d)$ and recombination correction factor k_s.

$$\mathrm{PDD}_c(d) = \frac{\mathrm{Q}_c(d)}{\mathrm{Q}_{c\_max}} = \frac{\mathrm{Q}_O(d) \cdot k_\mathrm{s}}{\mathrm{Q}_{c\_max}} \tag{4}$$

Considerable components of uncertainty for budget estimation are σ_{Q_O}, σ_{k_S} and $\sigma_{\mathrm{Q}_{C\_max}}$, so the measurement uncertainty of PDD measurement at certain depth (u_{Mes}) can be estimated from propagation of uncertainty as follows:

$$\begin{aligned} u_{Mes}^2 &= \left(\frac{\partial \mathrm{PDD}_C}{\partial \mathrm{Q}_O}\right)^2 u_{\mathrm{Q}_O}^2 + \left(\frac{\partial \mathrm{PDD}_C}{\partial k_S}\right)^2 u_{\mathrm{k}_S}^2 + \left(\frac{\partial \mathrm{PDD}_C}{\partial \mathrm{Q}_{c\_max}}\right)^2 u_{\mathrm{Q}_{C\_max}}^2 \\ &= \left(\frac{k_S}{\mathrm{Q}_{C\_max}}\right)^2 u_{\mathrm{Q}_O}^2 + \left(\frac{\mathrm{Q}_O}{\mathrm{Q}_{C\_max}}\right)^2 u_{\mathrm{k}_S}^2 + \left(-\frac{\mathrm{Q}_O \cdot k_S}{\mathrm{Q}_{C\_max}^2}\right)^2 u_{\mathrm{Q}_{C\_max}}^2 \end{aligned} \tag{5}$$

Here, u_{Q_O} and u_{k_S} at each measurement point were calculated from the standard deviation of repeated measurements. $u_{\mathrm{Q}_{C\_max}}$ at maximum measurement point was calculated from the standard deviation of repeated measurement as well. The uncertainty of k_s and P_{ion} were estimated from Eqs. (1) and (2). The potential uncertainty for estimating k_s and P_{ion} was assumed to be 0.1% in accordance with previous studies[8,13,20].

As for B-type uncertainty factors, uncertainty due to the measurement position, uncertainty due to temperature/pressure drift and potential uncertainty due to the ion recombination correction calculation are listed. As for the uncertainty due to the measurement position, the positional accuracy of the 3D water phantom (± 0.1 mm) and the water level change (0.1 mm) due to evaporation of water during measurement were taken into account; the change in measured values due to a positional change of 0.2 mm was calculated for each measurement position. In the PDD measurements, profile measurements were performed at an applied voltage of 300 V over approximately 15

minutes. When the applied voltage was changed to 100 V, after waiting 10 minutes for the measurements to stabilize, pre-dose irradiation was performed for 10 minutes (6 Gy) at a dose rate of 600 MU/min. The two PDD profile measurements at 300 V and 100 V took 15 minutes each, with a 20-minute wait for stabilization following the change in applied voltage, for a total of 50 minutes for one series of measurements. The uncertainty associated with temperature and pressure changes during PDD profile measurement was estimated to be 0.2%, assuming that the temperature change during the measurement was within 0.5°C and the pressure change varied within 1 hPa. Figure 11 (a) and (b) show the composite uncertainty at each measurement position for %DD(1) with negative and positive polarizing voltage. Figures 11 (c) and (e) show the same for %DD(2). The solid and open squares stand for the uncertainty for original PDD with resetup and repeat cases. The solid and open circles stand for the uncertainty for corrected PDD with resetup and repeat cases. The solid and open triangles stand for the uncertainty for k_s and P_{ion} with resetup and repeat cases. The solid line stands for the difference of corrected PDD from original PDD. As shown in Figure 11, although the composite uncertainty is large near the water surface, it becomes less than 0.2% at depths after 12 mm even in the case of resetup, indicating that estimation with sufficient accuracy is possible, including in the peak region.

5. CONCLUSIONS

We obtained depth profiles of 10 MV FFF beams using various ionization chambers and found that the deviation among these dosimeters amounted to 1%. This deviation occurs from the difference of DPP dependency of the ion collection efficiency for each ionization chamber. On the other hand, when the ion recombination correction was applied to the obtained depth profiles, the deviation was reduced from 1.0% to 0.5%. In this study, the deviation of PDD profile among the ionization chambers was reduced by the ion recombination coefficient including the DPP dependency, especially for high DPP beams such as FFF beams. The present method is particularly effective for CC13, where the ion collection efficiency is highly DPP dependent.

Conflict of Interest

The authors have no relevant conflicts of interest to disclose.

References

1. Palmans H, Andreo P, Huq MS, et al. Dosimetry of small static fields used in external photon beam radiotherapy: summary of TRS-483, the IAEA-AAPM international Code of Practice for reference and relative dose determination. *Med Phys.* 2019;45(11): 1123–1145.
2. KHAN, F.M., The Physics of Radiation Therapy. 5th edn. Lippincott Williams & Wilkins, Philadelphia, PA. 2014.
3. Fraass B, Doppke K, Hunt M, et al. American Association of Physicists in Medicine Radiation Therapy Committee Task Group 53: Quality assurance for clinical radiotherapy treatment planning. *Med Phys.*

1998;25:1773–1829.

4. Craig, T., D. Brochu, J. Van Dyk. A quality assurance phantom for three-dimensional radiation treatment planning. Int. *J Radiat Oncol Biol. Phys.* 1999;44(4):955–966.
5. Rangel A, Ploquin N, Kay I, Dunscombe P. Towards an objective evaluation of tolerances for beam modeling in a treatment planning system. *Phys Med Biol.* 2007;52(19):6011–6025.
6. Smilowitz JB, Das IJ, Feygelman V, et al. AAPM Medical Physics Practice Guideline 5.a.: commissioning and QA of treatment planning dose calculations – megavoltage photon and electron beams. *J Appl Clin Med Phys.* 2015;16(5):14–34.
7. Das IJ, Cheng CW, Watts RJ, et al. Accelerator beam data commissioning equipment and procedures: Report of the TG–106 of the Therapy Physics Committee of the AAPM. *Med Phys.* 2008;35(9):4186-4215.
8. Malcolm McEwen et al. Addendum to the AAPM's TG-51 protocol for clinical reference dosimetry of high-energy photon beams. *Med Phys.* 2014;41(4):041501.
9. K Derikum, M Roos. Measurement of saturation correction factors of thimble-type ionization chambers in pulsed photon beams. *Phys Med Biol.* 1993;38(6):755–763.
10. DT Burns, Malcolm McEwen. Ion recombination corrections for the NACP parallel-plate chamber in a pulsed electron beam. *Phys Med Biol.* 1998;43(8):2033–2045.
11. FD Martino, M Giannelli, et al. Ion recombination correction for very high dose-per-pulse high-energy electron beams. *Med Phys.* 2005;32(7):2204-2210.
12. G Bruggmoser, R Saum, et al. Determination of the recombination correction factor ks for some specific plane-parallel and cylindrical ionization chambers in pulsed photon and electron beams. *Phys Med Biol.* 2007;52(2):N35–N50
13. Malcolm McEwen et al. Measurement of ionization chamber absorbed dose k_Q factors in megavoltage photon beams. *Med Phys.* 2010;37(5):2179-2193.
14. Megan A. Hyun, Jessica R. Miller, et al. Ion recombination and polarity corrections for small-volume ionization chambers in high-dose-rate, flattening-filter-free pulsed photon beams. *Med Phys.* 2017;44(2):618–627.
15. Japan Society of Medical Physics . Standard Dosimetry of Absorbed Dose to Water in External Beam Radiotherapy. Tokyo: Tsusho‐sangyo‐kenkyusya; 2012.
16. Andreo P, Burns D T, et al. Absorbed Dose Determination in External Beam Radiotherapy. An International Code of Practice for Dosimetry Based on Standards of Absorbed Dose to Water. Technical Reports Series No. 398, International Atomic Energy Agency, Vienna. 2000.
17. J.W. BOAG, J. CURRANT. Current collection and ionic recombination in small cylindrical ionization chambers exposed to pulsed radiation. *Brit J Radiol*. 1980;53(629):471-478.
18. MS Weinhous, JA MELI. Determining Pion, the correction factor for recombination losses in an ionization chamber. *Med Phys.* 1984;11(6):846-849.
19. Almond PR, Biggs PJ, Coursey BM, et al. AAPM's TG-51 protocol for clinical reference dosimetry of high-energy photon and electron beams. *Med Phys.* 1999;26(9): 1847–1870.
20. Stephen F. Kry. Ion recombination correction factors (Pion) for Varian TrueBeam high-dose-rate therapy beams. *J Appl Clin Med Phys.* 2012;13(6):318-325.

21. F DeBlois, Corey Zankowski, et al. Saturation current and collection efficiency for ionization chambers in pulsed beams. *Med Phys.* 2000;27(5):1146-1155.
22. S Agostinelli, S Garelli, M Piergentili, et al. Response to high-energy photons of PTW31014 PinPoint ion chamber with a central aluminum electrode. *Med Phys.* 2008;35(7):3293-3301
23. J W Boag. Ionization measurements at very high intensities. *Brit J Radiol.* 1950;23(274):601–611.
24. J W Boag. The recombination correction for an ionization chamber exposed to pulsed radiation in a 'swept beam' technique. I. Theory. *Phys Med Biol.* 1982;27(2):201–211.
25. Martin Berg, Ole Noerrevang. Recombination factors for the cylindrical FC65-G ionization chamber in pulsed photon beams and the plane-parallel Roos ionization chamber in pulsed electron beams. *Phys Med Biol.* 2004;49(23):5309–5318.
26. J W Boag, E Hochhauser, O A Balk. The effect of free-electron collection on the recombination correction to ionization measurements of pulsed radiation. *Phys Med Biol.* 1996;41(5):885–897.
27. Z Chang, Q Wu, J Adamson, et al. Commissioning and dosimetric characteristics of TrueBeam system: Composite data of three True-Beam machines. *Med Phys.* 2012;39(11):6981–7018.
28. Y Tanaka, H Mizuno, Y Akino, et al. Do the representative beam data for TrueBeam linear accelerators represent average data? *J Appl Clin Med Phys.* 2019;20(2):51–62.
29. IJ Das, CF Njeh, CG Orton, et al. Vendor provided machine data should never be used as a substitute for fully commissioning a linear accelerator. *Med Phys.* 2012;39(2):569–572.
30. K Tani, A Wakita, N Tohyama, et al. Evaluation of differences and dosimetric influences of beam models using golden and multi-institutional measured beam datasets in radiation treatment planning systems. *Med Phys.* 2020;47(11):5852–5871.
31. Varian Medical Systems. Eclipse Photon and Electron Algorithms Reference Guide; 2019:P1026471-001-A.
32. Varian Medical Systems, personal communication.
33. Luis Brualla-González, Faustino Gómez, et al. Dose rate dependence of the PTW 60019 microDiamond detector in high dose-per-pulse pulsed beams. Phys Med Biol. 2016;61:N11–N19.
34. Sree Bash Chandra Debnath, Didier Tonneau et al. Dosimetric characterization of a small-scale (Zn,Cd)S:Ag inorganic scintillating detector to be used in radiotherapy. Physica Medica. 2021;84:15–23.

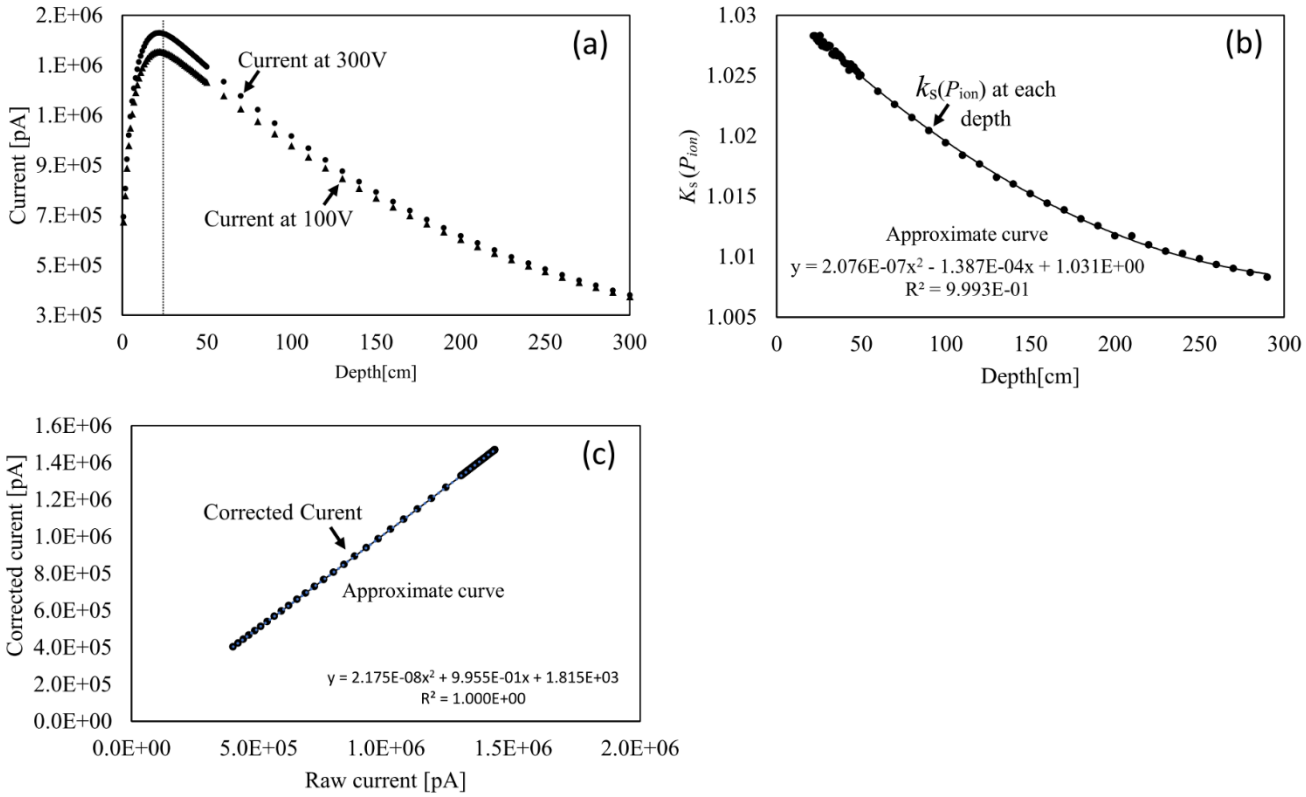

Figure 1. Figure 1. Methodology of ion recombination correction for PDD profile measurement

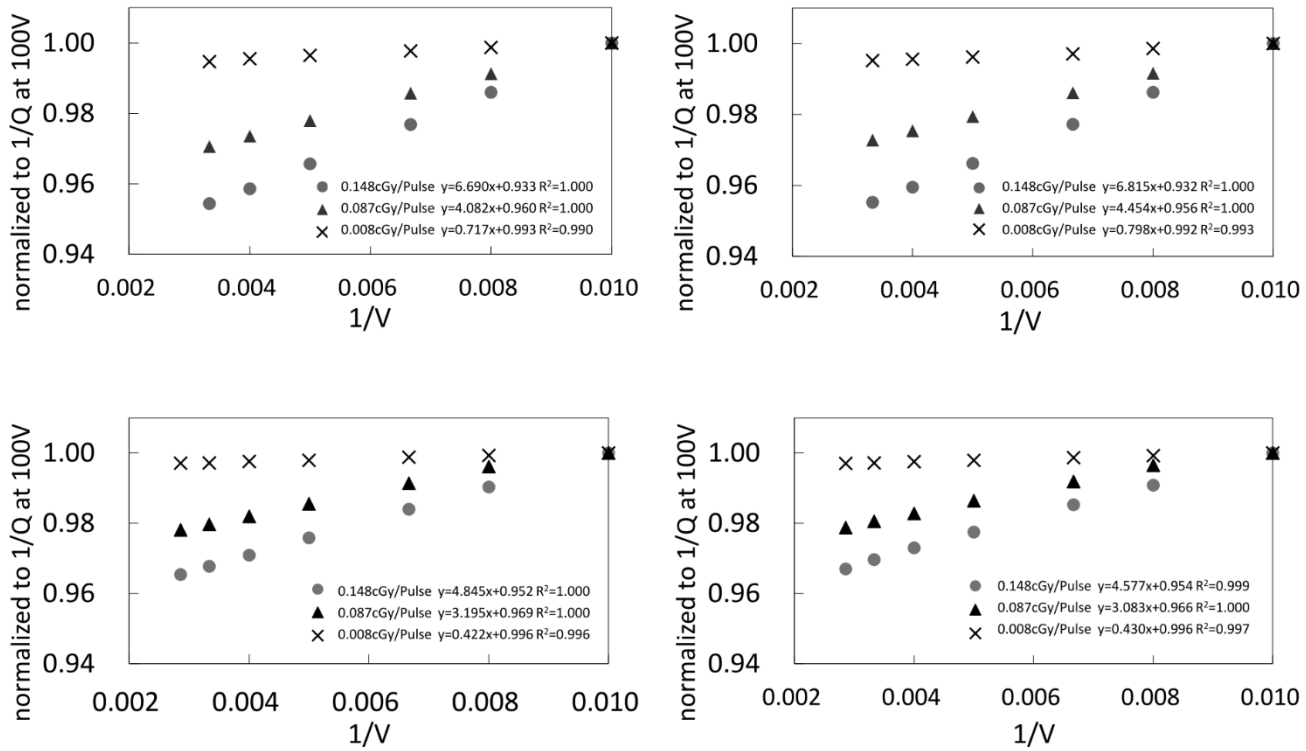

Figure 2. Jaffe-plots with DPP at 0.148, 0.087, 0.008 cGy/pulse for FC23-C and TN30013 chambers with positive and negative applied voltage.

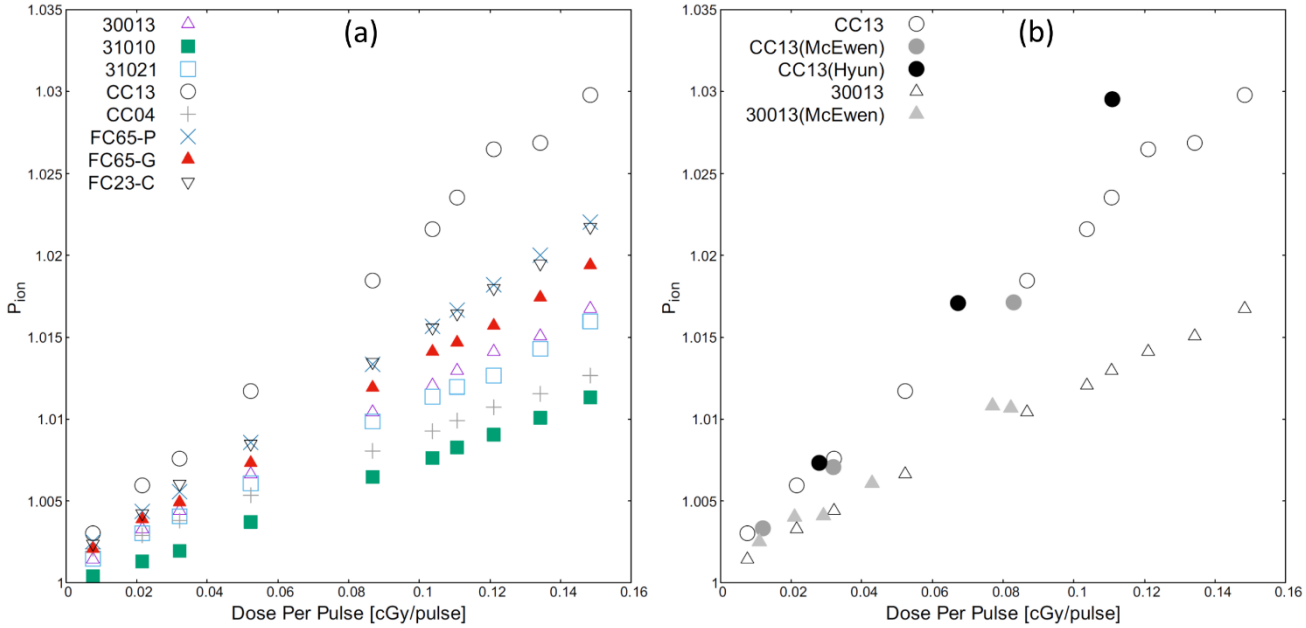

Figure 3. Relationship between DPP and ion recombination correction factor P_{ion} for ionization chambers. (a) all chambers, (b) 30013, CC13 compared with McEwen and Hyun.

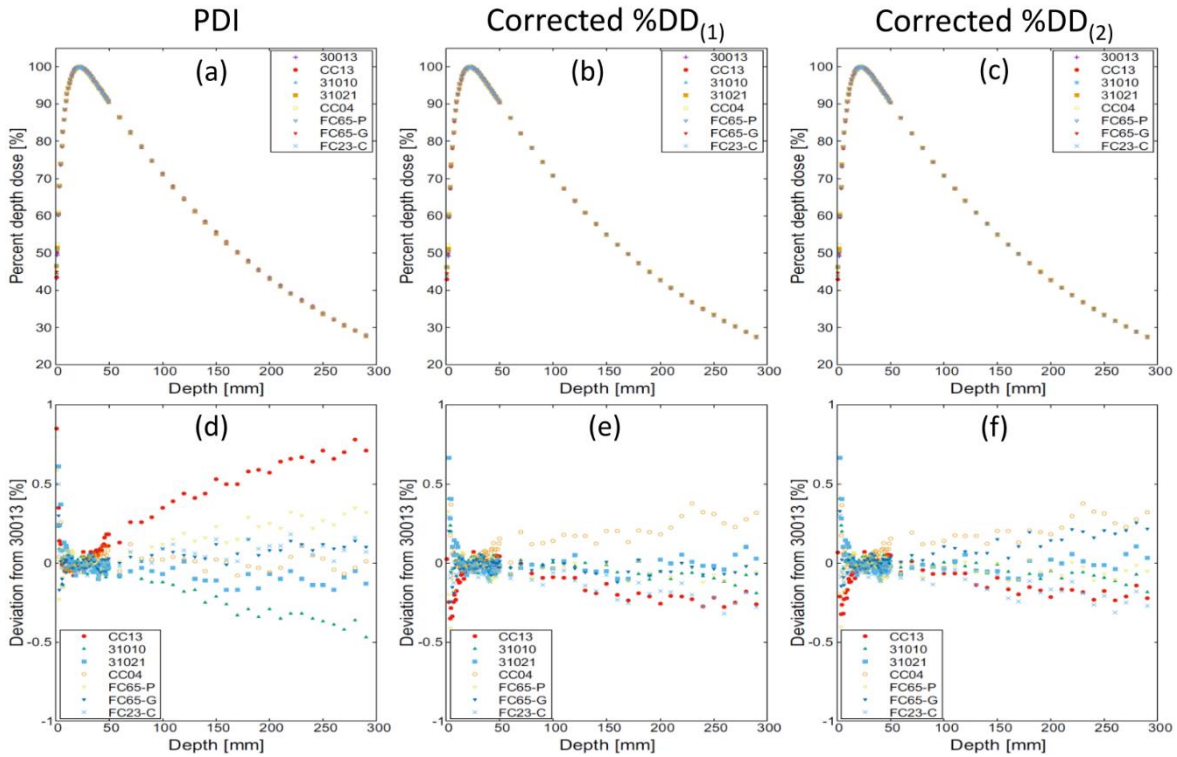

Figure 4. Original PDD and PDD with ion recombination correction by equations (1) and (2) at negative applied voltage. (a) original PDD normalized at maximum dose, (b) corrected $PDD_{(1)}$, (c) corrected $PDD_{(2)}$, (d) original PDD deviation from TN30013 for Farmer and mini-type, (e) corrected $PDD_{(1)}$ deviation from TN30013 for Farmer and mini-type, (f) corrected $PDD_{(2)}$ deviation from TN30013 for Farmer and mini-type.

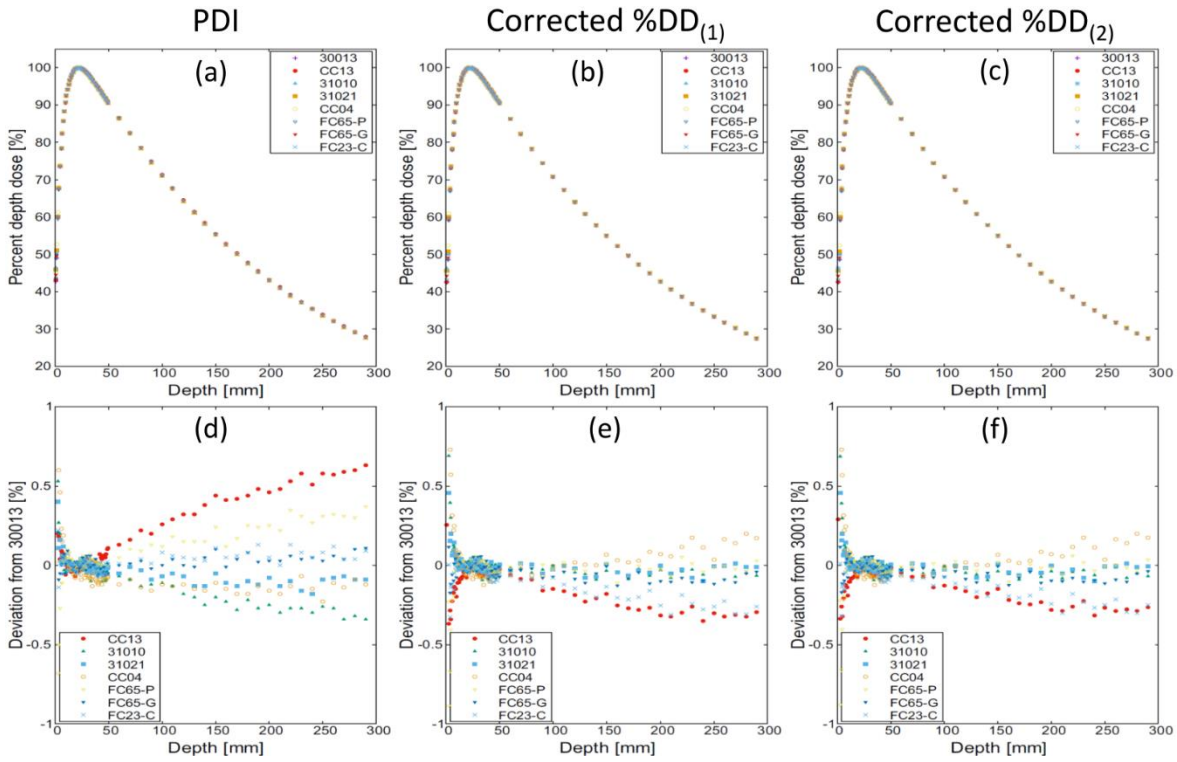

Figure 5. Original PDD and PDD with ion recombination correction by equations (1) and (2) at positive applied voltage. (a) original PDD normalized at maximum dose, (b) corrected $PDD_{(1)}$, (c) corrected $PDD_{(2)}$, (d) original PDD deviation from 30013 for Farmer and mini-type , (e) corrected $PDD_{(1)}$ deviation from 30013 for Farmer and mini-type , (f) corrected $PDD_{(2)}$ deviation from TN30013 for Farmer and mini-type.

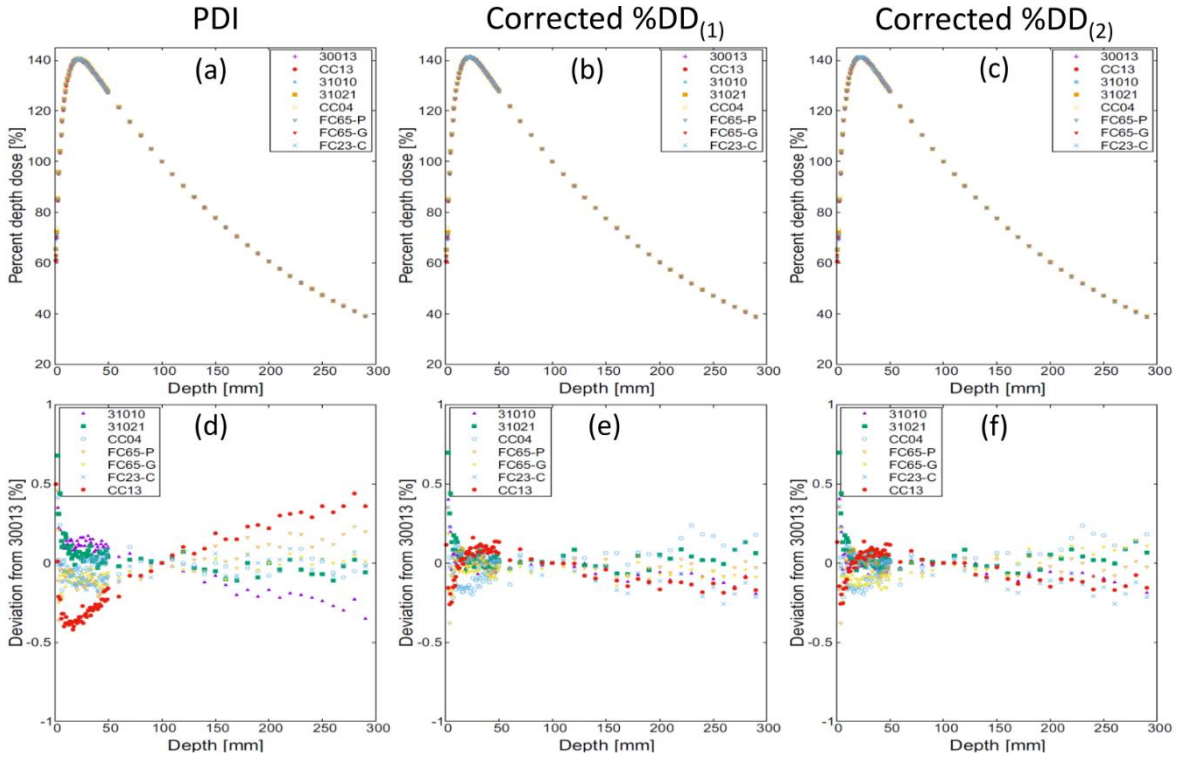

Figure 6. Original PDD and PDD normalized at 10 cm-depth with ion recombination correction by equations (1) and (2) at negative applied voltage. (a) original PDD normalized at 10 cm, (b) corrected $PDD_{(1)}$, (c) corrected $PDD_{(2)}$, (d) original PDD deviation from TN30013 for Farmer and mini-type , (e) corrected $PDD_{(1)}$ deviation from 30013 for Farmer and mini-type , (f) corrected $PDD_{(2)}$ deviation from 30013 for Farmer and mini-type.

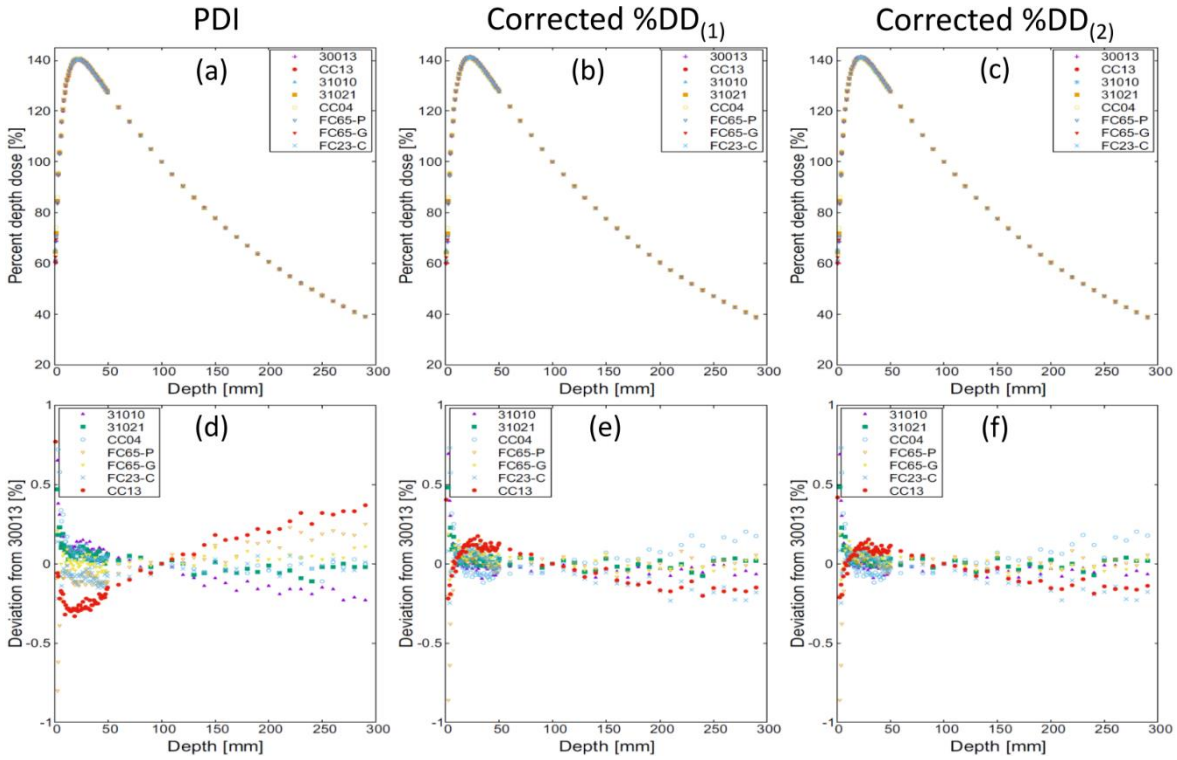

Figure 7. Original PDD and PDD normalized at 10 cm-depth with ion recombination correction by equations (1) and (2) at positive applied voltage. (a) original PDD normalized at 10 cm, (b) corrected $PDD_{(1)}$, (c) corrected $PDD_{(2)}$, (d) original PDD deviation from 30013 for Farmer and mini-type , (e) corrected $PDD_{(1)}$ deviation from 30013 for Farmer and mini-type , (f) corrected $PDD_{(2)}$ deviation from 30013 for Farmer and mini-type.

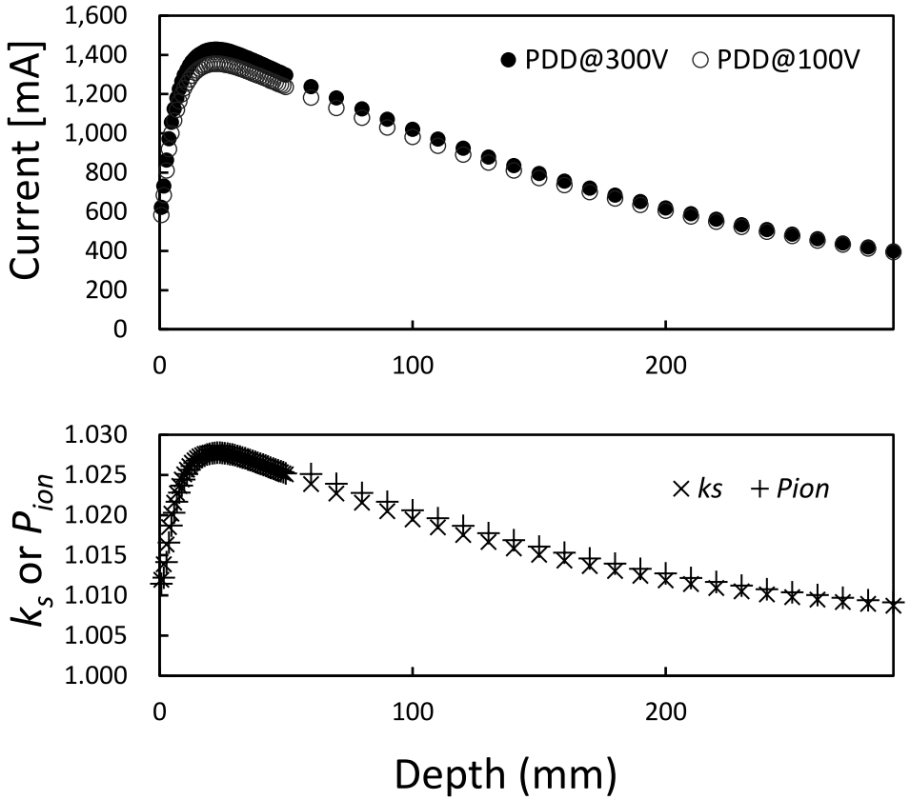

Figure 8. Depth-Current field at polarizing voltages of 100 and 300 V as a function of measurement depth associate with approximate k_s, P_{ion} for CC13 chamber.

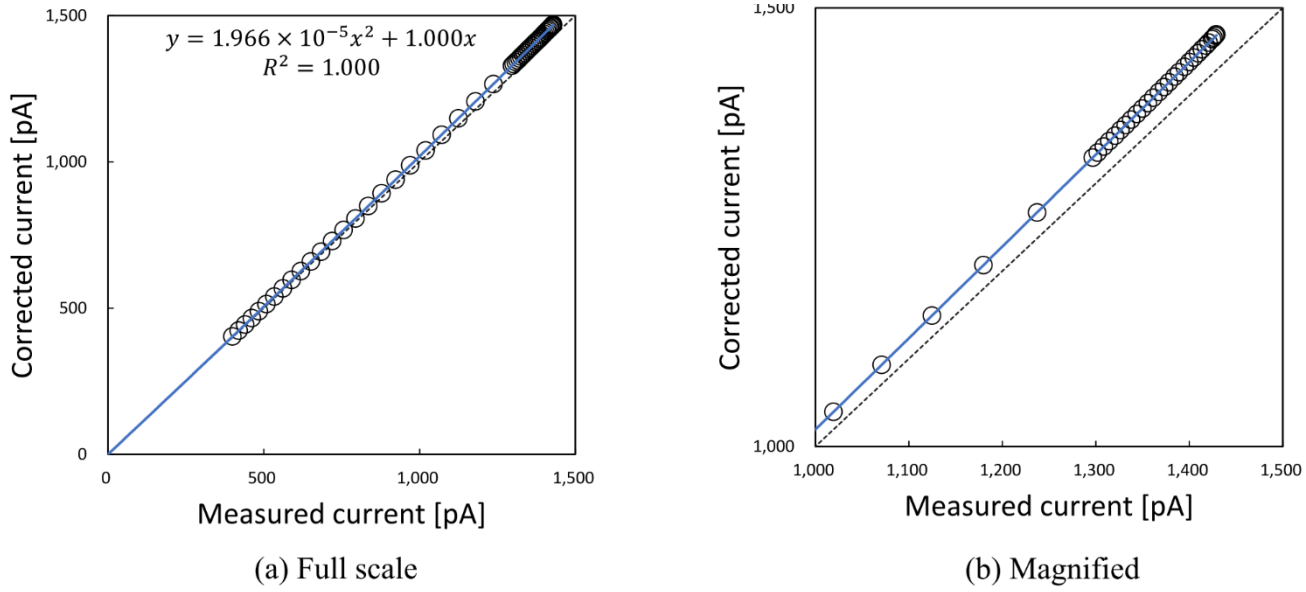

Figure 9. Relation between measured current and corrected current for CC13 chamber.

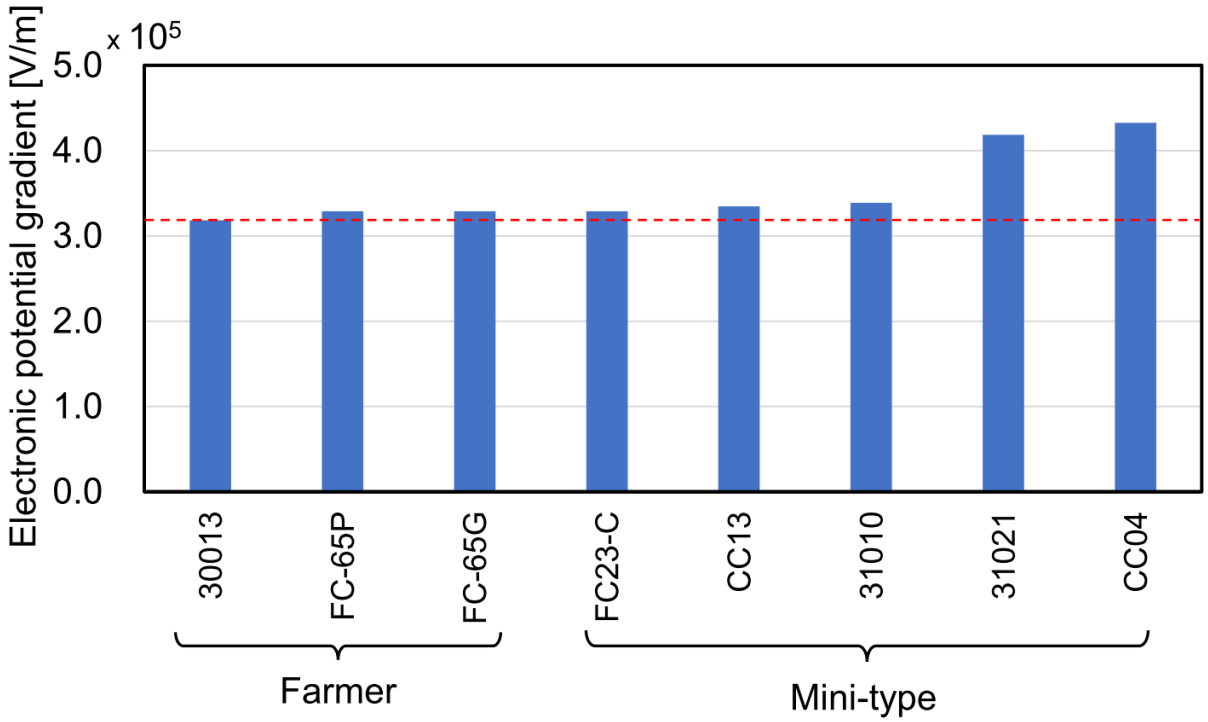

Figure 10. Electric potential gradient calculated from chamber dimensions.

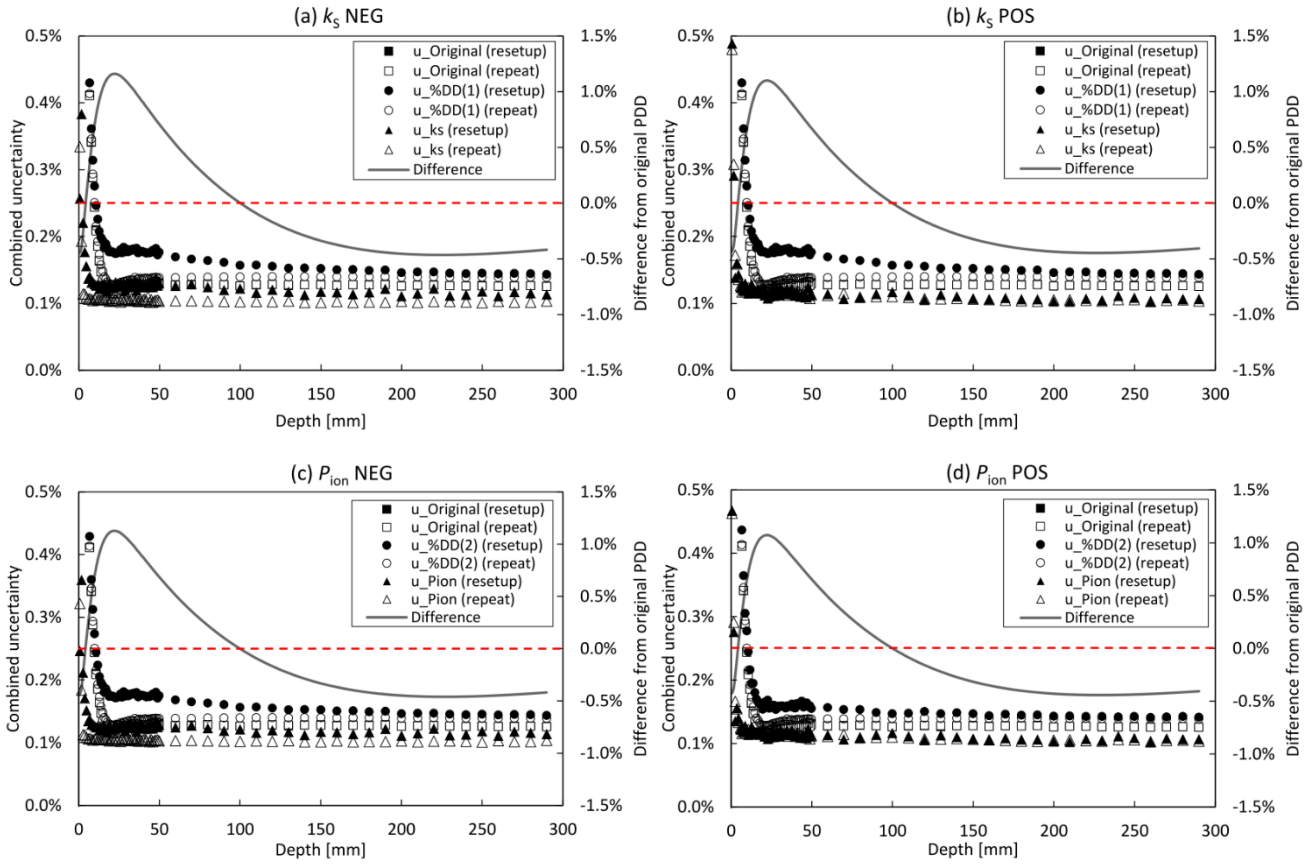

Figure 11. Combined uncertainty at each measurement point (k = 1).

Table 1. Irradiation settings for DPP (cGy/pulse) measurement.

Energy (MV)		4MV FF		6MV FF			10MV FFF				
Distance (cm)	SSD	90	90	100	100	100	90	100	100	90	90
	SCD	100	100	130	120	110	100	105	102.3	95	92.3
Depth (cm)		10	10	30	20	10	10	5	2.3	5	2.3
DPP(cGy/pulse)		0.008	0.022	0.032	0.052	0.087	0.104	0.111	0.121	0.134	0.148

Table 2. Characteristics of linear approximation for DPP dependency of P_{ion} obtained from Fig. 3(a).

	Chamber	POS			NEG		
		Slope	Intercept	R^2	Slope	Intercept	R^2
Farmer-type	30013	0.108	1.001	0.999	0.107	1.001	0.999
	FC65-P	0.139	1.001	1.000	0.146	1.001	1.000
	FC65-G	0.123	1.001	0.999	0.130	1.001	1.000
Mini-type	FC23-C	0.136	1.001	1.000	0.139	1.001	1.000
	CC13	0.194	1.002	0.996	0.207	1.001	0.999
	31010	0.078	1.000	0.999	0.075	1.002	0.999
	31021	0.101	1.001	0.999	0.098	1.001	0.995
	CC04	0.076	1.001	1.000	0.080	1.001	1.000

Table 3. Uncertainty budget for the corrected %DD.

Source	**Uncertainty Contribution**	**Type**
Measurement uncertainty (including setup)	u_{Mes}	A
Uncertainty for k_{s} or P_{ion}	$u_{k\mathrm{s}}$, $u_{P\mathrm{ion}}$	A
Potential uncertainty for estimating k_{s} or P_{ion}	0.1%	B
Position accuracy (including evaporation)	u_{Position}	B
Temperature / Pressure drift	0.196%	B